ISSN 1063-7788, Physics of Atomic Nuclei, 2022, Vol. 85, No. 3, pp. 282–288. © The Author(s), 2022. This article is an open access publication.
Russian Text © The Author(s), 2022, published in Yadernaya Fizika, 2022, Vol. 85, No. 3, pp. 209–215.

ELEMENTARY PARTICLES AND FIELDS
Experiment

Production of High-Transverse-Momentum Deuterons and Tritons at an Angle of 40° in Proton–Nucleus Interactions at a Beam Energy of 50 GeV

N. N. Antonov[1], V. A. Viktorov[1], V. A. Gapienko[1)*], G. S. Gapienko[1], V. N. Gres'[1], A. F. Prudkoglyad[1], V. A. Romanovskii[1], A. A. Semak[1], I. P. Solodovnikov[1], V. I. Terekhov[1], M. N. Ukhanov[1], and S. S. Shimanskii[2]

Received December 27, 2021; revised December 27, 2021; accepted January 5, 2022

Abstract—Data on the production of positively charged particles emitted at an angle of 40° (in the laboratory frame) with transverse momenta of up to 2.7 GeV/c in the interaction of 50-GeV/c protons with carbon, aluminum, copper, and tungsten nuclear targets are presented. Particular attention is given to studying the production of light nuclear fragments, such as deuterons (d) and tritons (t). An analysis of data on d and t particles gives grounds to state that these fragments arise via a local mechanism of their direct knockout from nuclei. The results were obtained in the SPIN experiment at the Institute for High Energy Physics (IHEP, Protvino).

DOI: 10.1134/S1063778822030036

The SPIN experiment studies the interaction of proton and carbon-nucleus beams extracted from the U-70 accelerator with nuclear targets (see, for example, [1–3]). The objective of these studies is to determine the inclusive spectra of secondary particles produced with high transverse momenta ($p_T >$ 1 GeV/c) in the cumulative region and to unearth, on this basis, the production mechanism for such particles. By the cumulative kinematical region, one usually means the region of momenta forbidden in kinematics for interactions on free nucleons. Although much data on cumulative processes have been accumulated over the past decades, the problem of the mechanisms of these processes remains open. Since cumulative effects manifest themselves only in interactions with nuclei, the structure of nuclear matter has not been understood conclusively. For the region of precumulative and cumulative processes involving high transverse momenta, there are virtually no data, while, according to the theoretical estimations presented in [4], a dominant contribution to these processes comes from hard interactions with intranuclear multinucleon (multiquark) configurations.

In the present article, we report on the results obtained by studying the production of deuterons (d) and tritons (t) emitted from targets at an angle of 40° (in the laboratory frame) in proton–nucleus interactions at the proton-beam energy of 50 GeV. The particle-emission angle chosen for the present measurements corresponds to an angle of about 150° with respect to the beam direction in the reference frame comoving with the center of mass of the incident proton and the intranuclear nucleon at rest.

The SPIN setup is a narrow aperture one-arm magnetic spectrometer consisting of seven magnetic elements, wire chambers, a a time-of-flight system, and a threshold Cherenkov detector. A description of the spectrometer can be found elsewhere [1]. Via changing the positions of the magnetic elements of the spectrometer arm, one can select charged particles emitted from the target at angles in the range of 22°–55° (in the laboratory frame). During the measurements, the magnetic optics of the spectrometer was tuned each time to the required momentum of the charged particle knocked out from the target. Thin plates from carbon, aluminum, copper, and tungsten were used as targets in the present study and in earlier studies of our group.

Our measurements were performed by employing a highly intense (about 2×10^{12} protons per second) proton beam extracted from the U-70 accelerator. The working range of secondary-particle momenta accessible at the chosen angle of the spectrometer arm was between 1 and 4.2 GeV/c. The momentum acceptance within this range is $\Delta p/p \approx 2\%$. The momentum itself was measured to a precision of $\sigma_p \sim 0.0025p$.

[1] Institute for High Energy Physics, National Research Center Kurchatov Institute, Protvino, Russia.
[2] Joint Institute for Nuclear Research, Dubna, Russia.
* E-mail: Vladimir.Gapienko@ihep.ru

The particles under study were identified on the basis of measurements of the time of flight over a base length of about 12 m. An example of the time-of-flight distribution for positively charged particles (π, K, p, d, and t) with momentum $p = 2.5$ GeV/c is given in Fig. 1 The distribution in this figure is raw one—not corrected for the efficiency of the propagation of various particles along the spectrometer arm. In plotting this figure, information coming from the threshold Cherenkov detector and making it possible to accomplish a reliable separation of π/K particles was not used either.

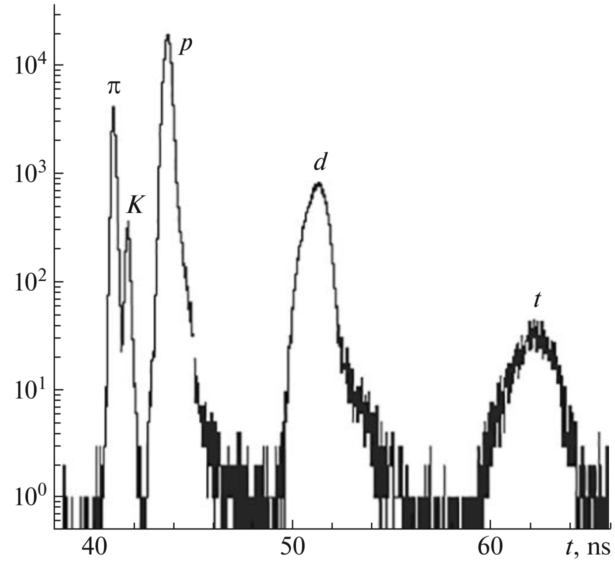

Fig. 1. Example of the time-of-flight distribution for particles of momentum $p = 2.5$ GeV/c.

For each pair of momentum and angular values to which the magnetic-spectrometer arm was tuned, the Geant4 code package [5] was used to calculate a table containing information about the propagation of a particle belonging to a specific type through the spectrometer. These tables were employed to reconstruct the inclusive cross sections from the primary data. The invariant cross sections for positively charged particles produced in proton interactions with carbon and tungsten targets are shown in Fig. 2 versus the particle momentum. The transverse-momentum values are given on the upper horizontal scales. The kinematical limit for nucleon–nucleon scattering at an angle of 40° is shown in both halves of Fig. 2 in the form the vertical dashed straight lines. Inspecting the spectra obtained for two different targets, one can reveal the following general regularities: As the momentum grows, the relative contribution of mesons decreases fast, while the contribution of d and t particles increases with respect to the proton yield. The behavior of the spectra measured with the other two target species, Al and Cu, exhibits the same features as the data in Fig 2 for carbon and tungsten nuclei. For carbon and tungsten targets, Fig. 3 shows the ratios of the (a) deuteron and (b) triton yields to the proton yield versus the transverse momentum. The results of the present measurements are given in this figure along with data obtained earlier in [3] for the d/p and t/p ratios with the same nuclei for a spectrometer angle of 35° (in the laboratory frame), at which the interval of momenta accessible to the measurements was broader than that at an angle of 40°. A comparison of data collected at different angles shows that, for a larger angle, the relative yield of d and t particles grows faster with increasing p_T.

In the experiment reported in [6], particle production at an angle of 15.9° (in the laboratory frame) in the interaction of 25-GeV protons with aluminum and platinum nuclei was studied at the CERN proton synchrotron (PS). The region of particle momenta measured in that experiment was $p \approx 2$–5 GeV/c, while the d/p ratio turned out to be a momentum-independent constant. This ratio was about 0.02 for the aluminum target and was about 1.5 higher than that for the platinum target.

In the FODS experiment at the U-70 accelerator (Protvino), the d/p ratio in proton–nucleus interactions at 70 GeV/c was measured in [7] for an emission angle of 9° (in the laboratory frame). The d/p ratio obtained in that experiment for the transverse-momentum range of $p_T = 1$–4 GeV/c turned out to be momentum-independent, in just the same way as in [6], and does not exceed 0.03 for all nuclei, including those of lead.

In contrast to the kinematical region studied by means of the SPIN setup, particle production was studied in [6, 7] for emission angles close to 90° in the reference frame comoving with the center of mass of the incident proton and the intranuclear nucleon involved at rest and without going beyond the kinematics of nucleon–nucleon interactions. The difference in the values and behavior of the d/p ratio between the data from the SPIN experiment and from the studies reported in [6, 7] may suggest that different mechanisms are responsible for the production of deuterons detected in those experiments.

The nucleon-coalescence model, according to which nucleons produced with close momenta may form nuclear fragments via coalescence (fusion), was proposed [8] in order to explain the appearance of nuclear fragments in interactions involving multiparticle production. In a simple form, the relation between the inclusive spectra of nucleons and a fragment of mass number A is specified by the coalescence coefficient

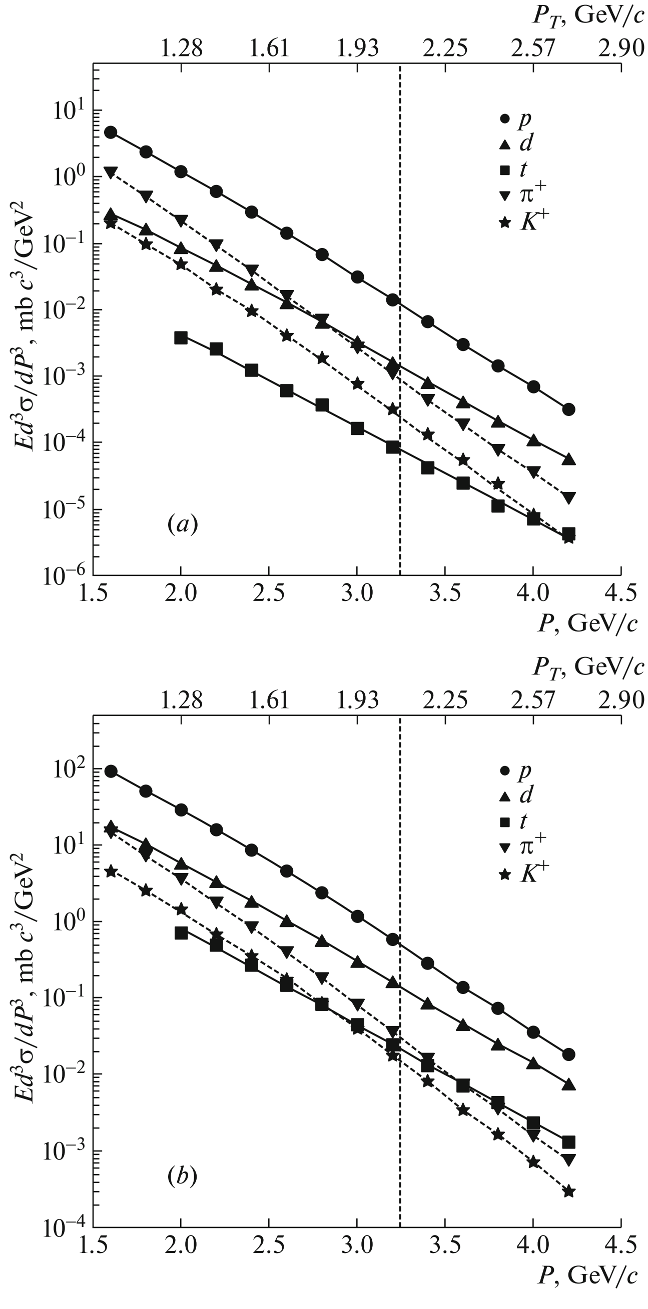

Fig. 2. Invariant cross sections for π^+, K^+, p, d, and t production at an angle of 40° in proton interactions with (a) carbon and (b) tungsten targets. The vertical lines correspond to elastic nucleon–nucleon scattering at an angle of 40°. The transverse-momentum values are given on the upper horizontal scale. The curves in this figure are drawn to guide the eye.

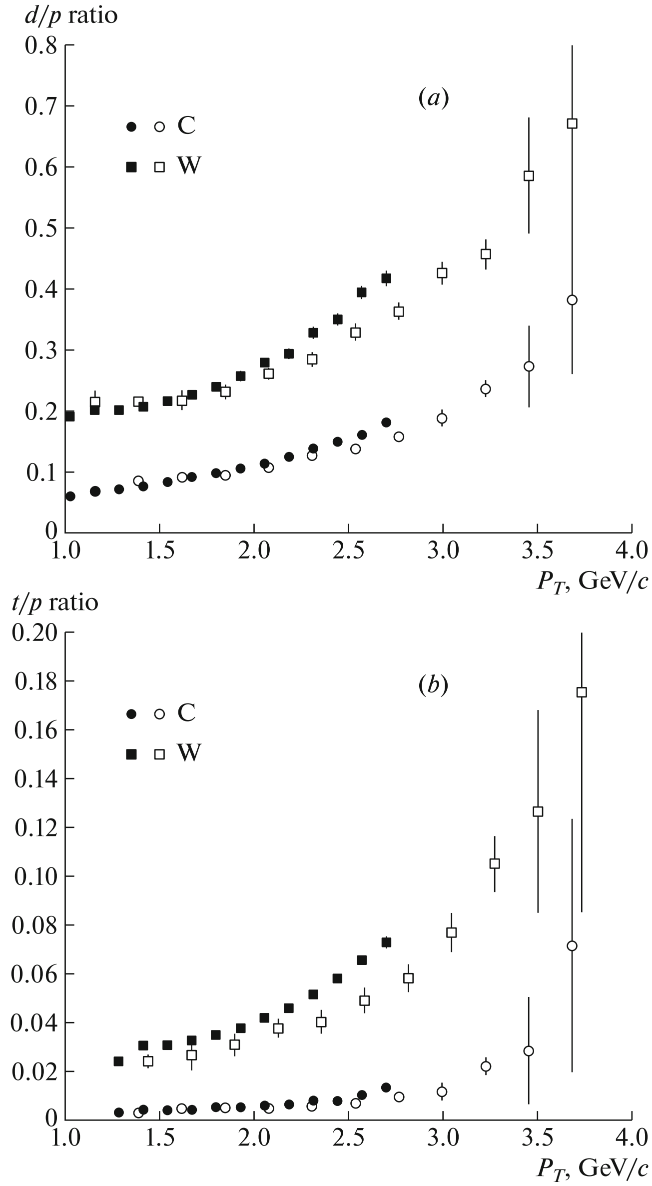

Fig. 3. Ratios of the (a) deuteron and (b) triton yields to the proton yield at various transverse momenta of particles in the cases of employing carbon and tungsten targets. The closed symbols represent results of the present study. The open symbols stand for data measured earlier in [3] for an angle of 35°.

B_A; that is,

$$\frac{E_A}{\sigma_{\rm inel}}\frac{d^3\sigma_A}{dp_A^3} = B_A\left(\frac{E_p}{\sigma_{\rm inel}}\frac{d^3\sigma_p}{dp_p^3}\right)^A. \qquad (1)$$

Here, the cross sections for the production of the proton and A fragment, σ_p and σ_A, are taken for identical momenta per nucleon—that is, the total momentum of the A fragment, p_A, is higher than the proton momentum p_p by the factor A. By $\sigma_{\rm inel}$, we mean the cross section for inelastic pA interaction. The coalescence model makes it possible to estimate the volume (V) of the region of nuclear-fragment formation. If a fragment of mass number A is produced, then the coalescence coefficient B_A is expressed in terms of the volume of fragment-formation region as follows: $B_A \sim V^{-(A-1)}$.

Expression (1) was written under the assumption that the inclusive cross sections for protons and neutrons are equal to each other. However, the neutron-to-proton ratio in nuclei grows with increasing mass number. For the production of, say, deuterons, the relation between the spectra should then take the form

$$\frac{E_d}{\sigma_{\text{inel}}}\frac{d^3\sigma_A}{dp_d^3} = B_2 K_{np}\left(\frac{E_p}{\sigma_{\text{inel}}}\frac{d^3\sigma_p}{dp_p^3}\right)^2, \qquad (2)$$

where K_{np} is the neutron-to-proton ratio in a given nucleus. The B_2 values extracted from relation (2) are given in Table 1. These values were obtained upon averaging over the deuteron-momentum interval between 2 and 4 GeV/c.

The values calculated for B_2 are typical values obtained for deuteron production in proton–nucleus and proton–proton interactions. Within quoted errors, there is no dependence of the measured coalescence coefficient on the radius of the nucleus—that is, the size of the region from which the pair of nucleons forming the deuteron originate is identical for all targets.

The short-range-correlation (SRC) model [9, 10], which assumes that, within nuclear matter, there exits a configuration of pointlike nucleons that are correlated at short distances and which have a high relative momentum but do not form bound states is one of the presently popular models intended for explaining the nature of cumulative processes. According to this model, the incident particle interacts with one nucleon from a correlated pair, whereas the second nucleon escapes from the nucleus as a spectator nucleon.

If the SRC mechanism is operative, then, at high momenta, the average baryon number should remain close to unity. Figure 4 shows the average baryon number $\langle N_{\text{bar}}\rangle$ as a function of the momentum. The quantity $\langle N_{\text{bar}}\rangle$ was determined as the ratio $(\sigma_p + 2\sigma_d + 3\sigma_t)/\sum\sigma_i$, where σ_p, σ_d, and σ_t are the cross sections for the production of protons, deuterons, and tritons, respectively, while $\sum\sigma_i$ is the sum of the cross sections for all measured positively charged particles. The observed excess of $\langle N_{\text{bar}}\rangle$ above unity as the momentum grows cannot be explained by the SRC mechanism.

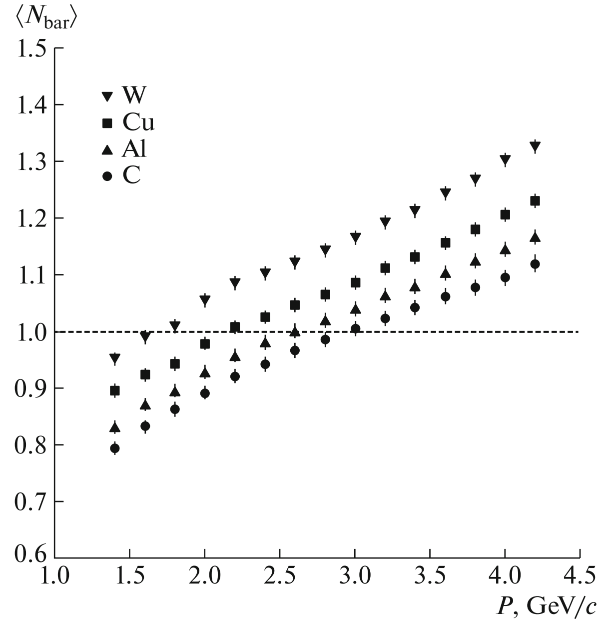

Fig. 4. Average baryon number at various momenta.

In a number of studies [4, 11, 12], it was assumed that, in reactions involving high transverse momenta, a dominant contribution comes from hard collisions between incident-hadron and target constituents. In order to describe the inclusive spectra of particles in the cumulative region and in the region of high transverse momenta, Stavinsky [13] proposed an algorithm that makes it possible to calculate quasibinary reactions in which constituents of colliding objects take part. For this purpose, he introduced the variables X_1 and X_2 (Stavinsky's variables) that describe those fractions of the primary 4-momenta of, respectively, the incident particle and target nucleus that are involved in collisions. For proton–nucleus interaction, X_1 values may range between 0 and 1, while X_2 values may change from 0 to A. In order to determine unambiguously the values of X_1 and X_2 in inclusive processes, Stavinsky supplemented the requirement of baryon-number conservation with the additional condition that the invariant energy of the quasibinary reaction takes a minimum value ($S_{\min}$).

The momentum spectra of deuterons and tritons measured in the SPIN experiments for four target species are shown in Fig. 5. The values calculated for Stavinsky's variable X_2 according to [13, 14] for deuterons and tritons are given on the upper horizontal scales of this figure. In the case being considered, X_2 is the minimum target mass (measured in nucleon-mass units) necessary for deuteron or triton production at an angle of 40°. As follows from the values on the upper scale in Fig. 5, the minimum target mass necessary for deuteron (triton) production should be greater than or equal to two (three) nucleon masses. Thus, it follows from the calculations that the observed production of d and t fragments proceeds through the interaction with a multinucleon (multiquark) object within the nucleus.

The analysis in [14, 15] of available experimental data on the production of high-p_T particles in the precumulative and cumulative regions shows that the invariant cross sections for particle production in

Table 1. Average values of B_2 for $p_d = 2$–4 GeV$/c$

Target	C	Al	Cu	W
B_2, GeV$^2/c^3$	0.021 ± 0.004	0.025 ± 0.004	0.029 ± 0.005	0.022 ± 0.003

interactions involving nuclei can be described by a dependence of the form

$$E\frac{d^3\sigma}{dp^3} = C_1 A_1^{\alpha(X_1)} A_2^{\alpha(X_2)} \exp(-\Pi/C_2), \quad (3)$$

where A_1 and A_2 the atomic masses of colliding nuclei, C_1 and C_2 are constants, Π is a dimensionless scaling variable of the form $\Pi = \sqrt{S_{\min}}/2m_N$, m_N is the nucleon mass, and $\alpha(X)$ is a function of X_1 or X_2.

Earlier [1], our group found that the best description of the pion-production spectra at an angle of 35° (in the laboratory frame) in proton–nucleus interactions at a momentum of 50 GeV$/c$ for the target species mentioned above was attained upon setting to $\alpha(X) = (2.45 + X)/3$ the power in the dependence on the nuclear mass in expression (3). In this form, this power-law dependence was used in the present study as well. The result of a simultaneous approximation of the deuteron and triton spectra by expression (3) is presented in Fig. 5 in the form of curves. The best description of the spectra is obtained upon setting the slope parameter to $C_2 = 0.172 \pm 0.003$ and the constants specifying the dimensionality of the cross section to $C_1 = 185 \pm 15$ mb c^3/GeV^2 for deuterons and to $C_1 = 56 \pm 13$ mb c^3/GeV^2 for tritons.

It is noteworthy that the variables X_1 and X_2 determined from the minimum value $S_{\min}$ cannot provide an exact description of the kinematics of quasibinary scattering, since the minimization proce-

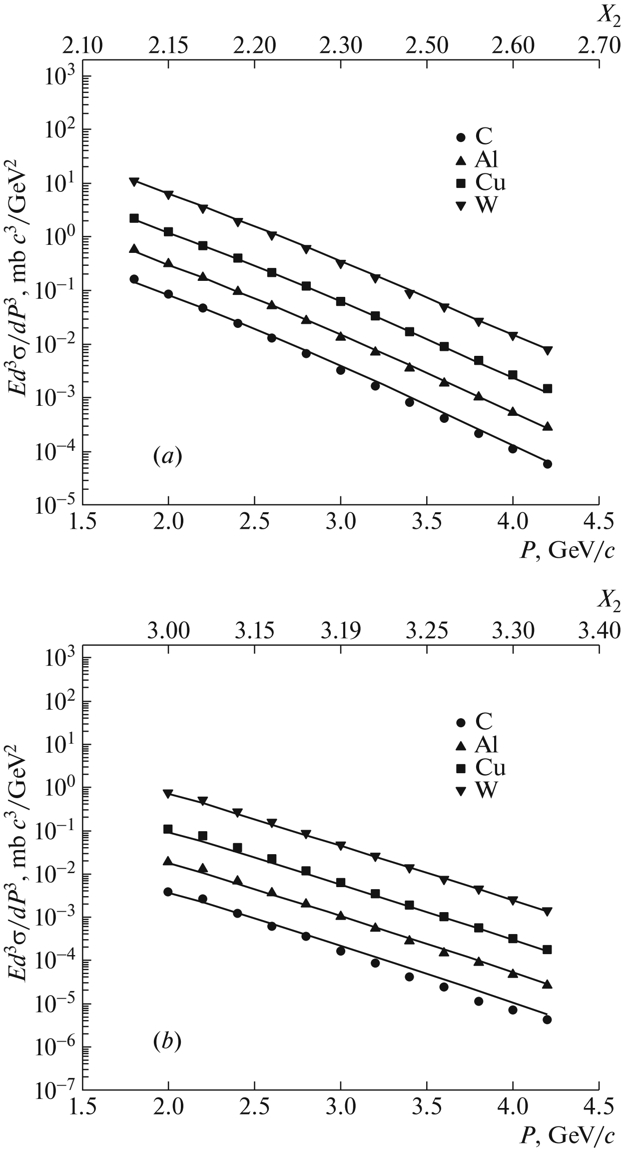

Fig. 5. Invariant cross sections for (*a*) deuteron and (*b*) triton production versus the momentum. The calculated values of the variable X_2 are given on the upper horizontal scales. The curves represent the results of an approximation of the data by a parameterization of the form (3).

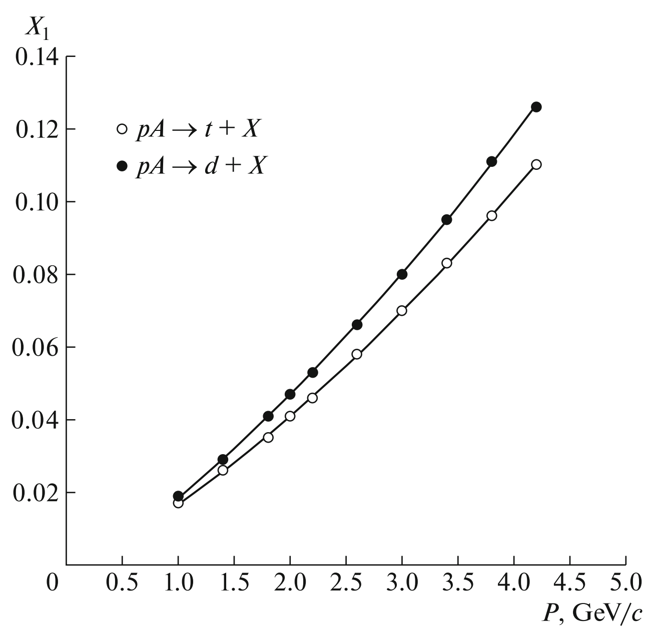

Fig. 6. Values calculated for Stavinsky's variable X_1 for d and t production according to the algorithm proposed in [14] for various values of the fragment momentum.

dure takes no account of the projectile and target structure functions. Nevertheless, good agreement of the parametrization in (3) and our experimental data favors the production of d and t particles via hard collisions involving intranuclear deuteron- and triton-like objects.

The idea that lower mass nuclei in a compressed state exist in nuclear matter was put forth by Blokhintsev [16] in order to explain experimental data from [17] on the knockout of light nuclear fragments from nuclei. In [17] deuteron production was considered as the result of elastic scattering of a primary proton with energy 675 MeV off a quasideuteron cluster within the nucleus, but, in our case, only proton constituents take part in hard scattering that leads to the appearance of high-p_T d and t particles. Figure 6 shows the calculated values of that fraction of the incident-proton 4-momentum which is sufficient for the production of a given nuclear fragment at an angle of 40°.

CONCLUSIONS

Inclusive spectra of positively charged particles produced with transverse momenta of up to 2.7 GeV/c at an angle of 40° in proton–nucleus interactions at a beam energy of 50 GeV have been measured. These spectra obtained with four different targets (carbon, aluminum, copper, and tungsten ones) exhibit the same regularities: as the momentum grows, the relative contribution of mesons decreases fast, while the contributions of d and t particles increases with respect to the proton yield.

A strong difference has been revealed in the values and in the behavior of the d/p ratio between the data from the SPIN experiment and the data obtained in the investigations reported in [6, 7], where the angle of particle production in proton–nucleus interactions corresponded to an angle of 90° in the reference frame comoving with the center of mass of the incident proton and intranuclear nucleon involved.

The application of the nucleon-coalescence model to deuteron production has shown that, within the errors, the region of emission of deuteron constituents has the same size for all of the targets used.

Our data on d and t particles cannot be explained within the SRC model [9, 10], where, because of short-range correlations, intranuclear nucleons may be at short distances without forming bound states. The interaction of a projectile particle with such a configuration of correlated intranuclear nucleons cannot lead to the appearance of fast nuclear fragments.

The spectra of d and t fragments are well described by expression (3) with the same form of dependence on the mass of the nucleus and the same slope parameter. Expression (3) is based [14, 15] on the model that treats the production of high-p_T particles as the result of a hard collision between a constituent of the incident particle and the target. According to the calculations reported in [14], a mass of about two (three) nucleon masses is an optimum target mass that is necessary, in the case being considered, for deuteron (triton) production at an angle of 40°. This suggests that the SPIN experiment detects d and t fragments produced via their direct knockout from nuclei.

ACKNOWLEDGMENTS

We are indebted to the headquarters of Institute for High Energy Physics, National Research Center Kurchatov Institute, for support of this investigation and to personnel of the Accelerator Department and Beam Department for providing efficient operation of the U-70 accelerator and eighth beam channel.

We are grateful to Professor A.M. Zaitsev for carefully reading the manuscript of the articles and for a number of critical comments that permitted improving the quality of presentation of our data.

Thanks are also due to A.T. Golovin for his invaluable technical support in the preparation of the SPIN setup for performing measurements.

OPEN ACCESS

REFERENCES

1. V. V. Ammosov, N. N. Antonov, V. A. Viktorov, V. A. Gapienko, G. S. Gapienko, V. N. Gres', V. A. Korotkov, A. I. Mysnik, A. F. Prudkoglyad, Yu. M. Sviridov, A. A. Semak, V. I. Terekhov, V. Ya. Uglekov, M. N. Ukhanov, B. V. Chuiko, A. A. Baldin, and S. S. Shimanskii, Yad. Fiz. Inzhin. **4**, 773 (2013).

2. N. N. Antonov, V. A. Viktorov, V. A. Gapienko, G. S. Gapienko, V. N. Gres', M. A. Ilyushin, V. A. Korotkov, A. I. Mysnik, A. F. Prudkoglyad, A. A. Semak, V. I. Terekhov, V. Ya. Uglekov, M. N. Ukhanov, B. V. Chuiko, and S. S. Shimanskii, JETP Lett. **101**, 670 (2015).
3. N. N. Antonov, A. A. Baldin, V. A. Viktorov, V. A. Gapienko, G. S. Gapienko, V. N. Gres', M. A. Ilyushin, V. A. Korotkov, A. I. Mysnik, A. F. Prudkoglyad, F. F. Semak, V. I. Terekhov, V. Ya. Uglekov, M. N. Ukhanov, B. V. Chuiko, and S. S. Shimanskii, JETP Lett. **104**, 662 (2016).
4. A. V. Efremov, V. T. Kim, and G. I. Lykasov, Sov. J. Nucl. Phys. **44**, 151 (1986).
5. J. Allison, K. Amako, J. Apostolakis, P. Arce, M. Asai, T. Aso, E. Bagli, A. Bagulya, S. Banerjee, G. Barrand, B. R. Beck, A. G. Bogdanov, D. Brandt, J. M. C. Brown, H. Burkhardt, Ph. Canal, et al., Nucl. Instrum. Methods Phys. Res., Sect. A **835**, 186 (2016).
6. V. T. Cocconi, T. Fazzini, G. Fidecaro, M. Legros, N. H. Lipman, and A. W. Merrison, Phys. Rev. Lett. **5**, 19 (1960).
7. V. V. Abramov et al., Sov. J. Nucl. Phys. **45**, 845 (1987).
8. S. T. Butler and C. A. Pearson, Phys. Rev. Lett. **7**, 69 (1961); Phys. Rev. **129**, 836 (1963).
9. M. I. Strikman and L. L. Frankfurt, Sov. J. Part. Nucl. **11**, 221 (1980).
10. J. Arrington, D. W. Higinbotham, G. Rosner, and M. Sargsian, Prog. Part. Nucl. Phys. **67**, 898 (2012).
11. L. P. Kaptar', B. L. Reznik, and A. I. Titov, Sov. J. Nucl. Phys. **42**, 492 (1985).
12. V. K. Luk'yanov and A. I. Titov, Sov. J. Part. Nucl. **10**, 321 (1979).
13. V. S. Stavinsky, JINR Rapid Comm. **18**, 5 (1986).
14. A. A. Baldin, JINR Rapid Comm. **3** (54), 27 (1992).
15. A. A. Baldin, E. N. Kladnitskaya, and O. V. Rogachevsky, JINR Rapid Comm. **2** (94), 20 (1999).
16. D. I. Blokhintsev, Sov. Phys. JETP **6**, 995 (1957).
17. L. S. Azhgireĭ, I. K. Vzorov, V. P. Zrelov, M. G. Meshcheryakov, B. S. Neganov, and A. F. Shabudin, Sov. Phys. JETP **6**, 911 (1957).